



ELSEVIER

Available online at www.sciencedirect.com

SCIENCE @ DIRECT®

Journal of Magnetism and Magnetic Materials 300 (2006) 471–478



www.elsevier.com/locate/jmmm

Magnetic properties of Co–Pt alloy nanowire arrays in anodic alumina templates

T.R. Gao^a, L.F. Yin^a, C.S. Tian^a, M. Lu^b, H. Sang^b, S.M. Zhou^{a,b,*}

^aSurface Physics Laboratory (National Key Laboratory) and Department of Physics, Fudan University, Shanghai 200433, China

^bState Key Laboratory of Solid State Microstructures, Nanjing University, Nanjing 210093, China

Received 15 October 2004; received in revised form 30 May 2005

Available online 1 July 2005

Abstract

Microstructure and magnetic properties of ferromagnetic Co₉Pt nanowire arrays electrodeposited into self-assembled anodic alumina templates have been investigated. X-ray diffraction shows that as-prepared Co–Pt nanowires are of FCC polycrystalline structure. The nanowires with diameter $d < 80$ nm are mainly of (1 1 1) preferred orientation along the wire axis. For a specific diameter, the coercivity and the remanent ratio with the external magnetic field parallel to the nanowire axis, i.e., the parallel geometry, are larger than those of the perpendicular geometry. With temperature increasing from 90 to 600 K, above two physical quantities in the perpendicular geometry decrease monotonically, while those of the parallel geometry change little. The dependence of the coercivity and the remanent ratio on temperature and the nanowire diameter can be explained after the shape and the magnetocrystalline anisotropies, and the dipolar magnetic interaction are considered. For the parallel and perpendicular geometries, the coercivity decreases with increasing diameter d as a linear scale of $1/d^2$ and approaches each other in the two geometries for large d . The degradation of coercivity in Co–Pt nanowires with increasing diameter is suggested to come from the curling mode of magnetization reversal process.

© 2005 Elsevier B.V. All rights reserved.

PACS: 75.50.-y; 75.60.-d; 75.75.+a

Keywords: Nanowire; Coercivity; Curling mode; Magnetocrystalline anisotropy

1. Introduction

Porous anodic alumites are considered as particularly attractive template materials for fabrication of nanowires, because the pore density is high, the pore distribution is uniform and the

*Corresponding author. Physics Department, 220 Handan road, Shanghai 200433, PR China. Tel.: +862165642316; fax: +862165104949.

E-mail address: shimingzhou@yahoo.com (S.M. Zhou).

diameter of the pores is small [1,2]. Due to the shape anisotropy, the magnetic easy axis will be aligned along the magnetic nanowires with strong perpendicular magnetic anisotropy if the wire length is much larger than its diameter. Therefore, the magnetic nanowire arrays are expected to have great potential applications in high-density perpendicular magnetic recording [3]. Many kinds of magnetic metals and alloys, such as Fe, Co, Ni, and their alloys Fe–Co and Fe–Ni have been prepared by electro-deposition into self-assembled anodic alumina oxide (AAO) templates [4–10]. For magnetic nanowire arrays, microstructure, magnetic interaction, and magnetization reversal process have been studied extensively. For most nanowires, the squareness of hysteresis loops along the nanowire axis, i.e., the parallel geometry, is far below one unit despite large shape anisotropy. Two possible reasons have been proposed. First, the magnetostatic interaction between neighboring wires has a serious influence on the magnetization reversal process of magnetic nanowires. Secondly, in addition to the shape anisotropy, the magnetocrystalline anisotropy also has an influence on the magnetization reversal process. If the easy axis of the magnetocrystalline anisotropy is not aligned along the nanowire axis, the squareness along the nanowire will be reduced. It is noted that attention has recently been focused on the magnetocrystalline anisotropy of nanowires and on the correlation between the microstructure and the magnetic properties. Therefore, studies of the coercivity in the parallel and perpendicular geometries are required.

Cobalt–platinum alloys have been extensively studied because of importance in both basic research and potential applications [11–16]. First, well-known, single-phased, disordered Co–Pt alloys can be formed in a wide composition range. For some specific compositions, the transformation from disorder to order has been observed after annealing at high-temperatures [11]. Secondly, disordered and ordered Co–Pt alloys are easy to have perpendicular anisotropy and the latter ones can have magnetic perpendicular anisotropy as large as about 4×10^7 erg/cm³ [12]. Thirdly, the Co–Pt alloy films have large polar Kerr effect at short wavelengths [13]. Finally, they

have good chemical stability and good corrosion resistance [14]. Therefore, Co–Pt alloys have potential applications in the fields of magneto-optical and magnetic storage. In this paper, we report on preparation of Co–Pt nanowires and their magnetic properties. Up to now, few reports have appeared on fabrications of Co–Pt alloy nanowires [11,15,16]. The evolution of the microstructure and the magnetic properties of Co–Pt nanowires with diameter and temperature was studied.

2. Experimental

Co₉Pt nanowires 3- μ m long with different diameters were prepared by electrodeposition. In order to prepare AAO templates, high purity (99.99%) Al sheets were first ultrasonically degreased in trichloroethylene and then etched in NaOH. Subsequently, the sheets were electropolished for 3 min in a mixed solution of C₂H₂O₆ and HClO₄ (volume ratio = 4:1). Then they were anodized in different acidic solution such as 1.2 M sulfuric acid and 0.6 M oxalic acid for 60 min. After the completion of AAO templates, the electrodeposition was conducted at 200 Hz and 13 V AC at room temperature for a duration of 5 min by using graphite as the counter-electrode. The Co and Pt atoms were electrodeposited into templates from an aqueous bath containing 2 g/L H₂PtCl₆ · 6H₂O and 11.2 g/L CoSO₄ · 7H₂O. 30 g/L boric acid was added to adjust the pH value to 5.0. The composition of the Co–Pt nanowires was adjusted by varying the volume ratio of the H₂PtCl₆ · 6H₂O and CoSO₄ · 7H₂O solutions. With atomic absorption spectroscopy (AAS), the Co content of the Co–Pt nanowire was found to be about 90 at%. In this study, transmission electron microscopy (TEM) was used to determine the morphology of AAO films, as well as topography, diameter, and length of nanowires. The microstructural characterization of nanowires was performed by X-ray diffraction (XRD). The magnetic properties of the arrays at various temperatures were measured using vibrating sample magnetometer (VSM) with a maximum external magnetic field of 1.0 T.

3. Results and discussion

Fig. 1(a) shows a plan-view TEM micrograph of oxalic-acid anodized AAO template sample with 30 V DC for 60 min. Highly ordered nanohole arrays were formed with an average diameter of 40 nm. In experiments, the average diameter of the pores was found to increase linearly with anodizing voltage. For further TEM measurements, Co–Pt nanowires were liberated from the AAO

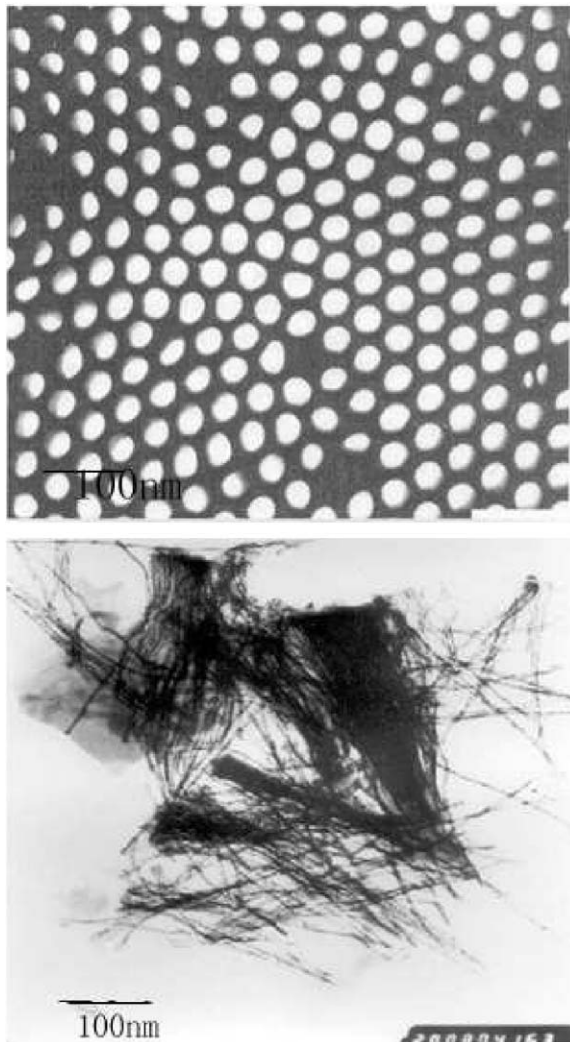


Fig. 1. (a) Plan-view TEM micrograph of an AAO template with 40 nm diameter holes. (b) TEM image of Co–Pt nanowires liberated from AAO template.

film by dissolving the alumina layer with aqueous NaOH. Co–Pt nanowires were found to be not smooth and not very uniform along the nanowire with an average length of about 3- μm , as shown in Fig. 1(b).

Before X-ray measurements, Al substrates were removed from the AAO films by using aqueous HgCl_2 to avoid the influence of the Al substrate. Co–Pt nanowires are still kept in the AAO templates, which have flat surfaces. Fig. 2 shows the XRD spectra of aligned Co–Pt nanowires in the AAO film with different diameters. The spectra clearly indicate that Co–Pt nanowires have FCC structure with preferred texture orientations of (1 1 1), (2 0 0), and so on along the wire axis. For nanowires with $d < 80$ nm, the intensity of the (1 1 1) peak is much larger than those of others and the lattice constant $a_0 = 3.33$ Å for Co–Pt nanowires. For the diameter of 80 nm however, the diffraction peaks of (0 0 1), (1 1 0), (2 0 0), and (2 2 0) become stronger in comparison with small diameters, showing a more random distribution of grain orientations. Moreover, Co(1 1 1) diffraction peak was detected at $2\theta = 44.4^\circ$. In order to verify a homogeneous distribution in composition and structure for $d < 80$ nm, more experiments are required.

Hysteresis loops were measured at various temperatures for nanowires with various diameters in the parallel and perpendicular geometries. Fig. 3 presents typical hysteresis loops for Co–Pt nanowires with a diameter of 60 nm in the temperature range 90–600 K. For the present sample, the coercivity and the squareness in the parallel geometry are much larger than those of the perpendicular geometry. The coercivity in the two geometries tends to approach each other at low temperatures.

Fig. 4 shows the coercivity in the parallel and the perpendicular geometries $H_C(\parallel)$ and $H_C(\perp)$, and remanent ratio $M_r/M_s(\parallel)$ and $M_r/M_s(\perp)$ as a function of temperature. In Fig. 4(a), $H_C(\perp)$ decreases monotonically and $H_C(\parallel)$ does not decrease monotonically as T increases, which is in accordance with report by Paulus et al. [17]. $\Delta H_C = H_C(\parallel) - H_C(\perp)$ increases with increasing temperature. As shown in Fig. 4(b), along the parallel direction the remanent ratio $M_r/M_s(\parallel)$

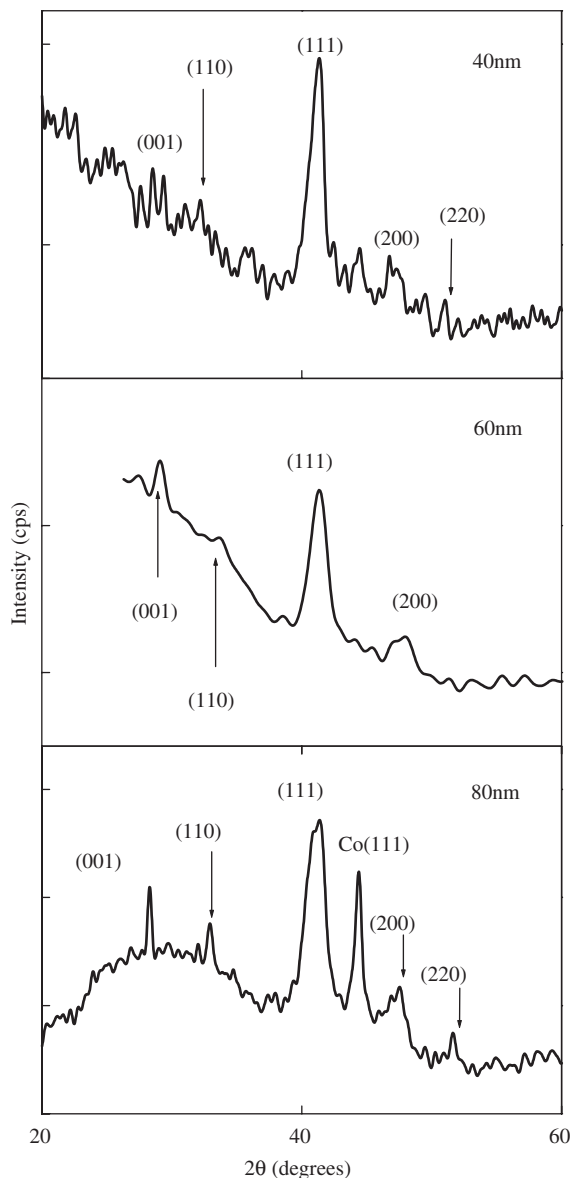


Fig. 2. X-ray diffraction patterns of AAO films filled with aligned Co–Pt nanowires with diameters of (a) 40 nm, (b) 60 nm, and (c) 80 nm. All diffraction peaks belong to Co–Pt, except for Co (111) in (c).

increases with the temperature increasing while $M_r/M_s(\perp)$ in perpendicular geometry decreases. This indicates that the magnetic easy axis turns away from the nanowire axis at low temperatures.

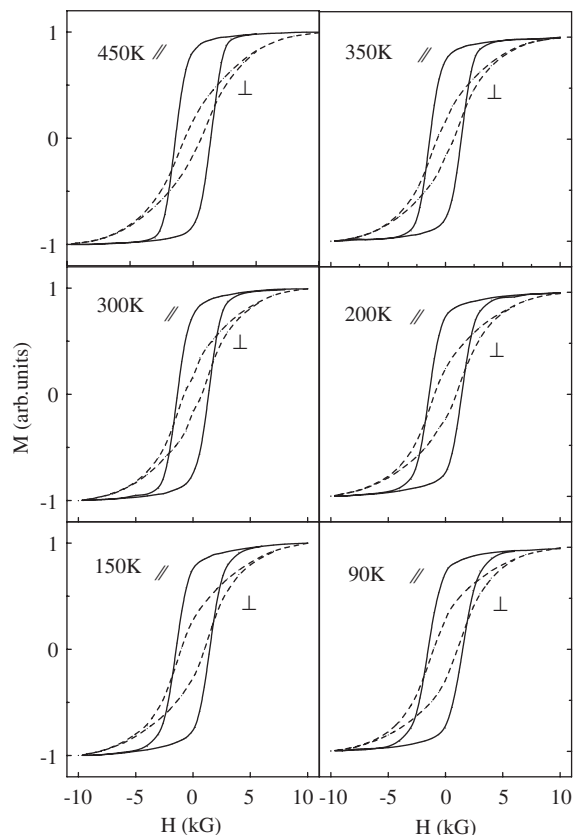


Fig. 3. Magnetization hysteresis loops for an array of 60 nm diameter Co–Pt nanowires in AAO template at different temperatures. The solid and dash curves refer to the external magnetic field parallel and perpendicular to the wire axis, respectively.

Fig. 5 presents typical hysteresis loops for Co–Pt nanowires with the diameters of 40 and 80 nm at room-temperature. For the diameter of 40 nm, the coercivity in the parallel geometry is larger than that of the perpendicular geometry and the coercivity in the two geometries approaches each other for the diameter of 80 nm. For diameters of 40 and 80 nm however, the squareness in the parallel geometry is larger than that of the perpendicular geometry. Similar phenomena were also observed in other kinds of nanowires and attributed to the parallel alignment of the magnetic easy axis along the wire axis [4–10]. Therefore, for Co–Pt nanowires with small diameters, the easy axis of magnetic anisotropy favors to be

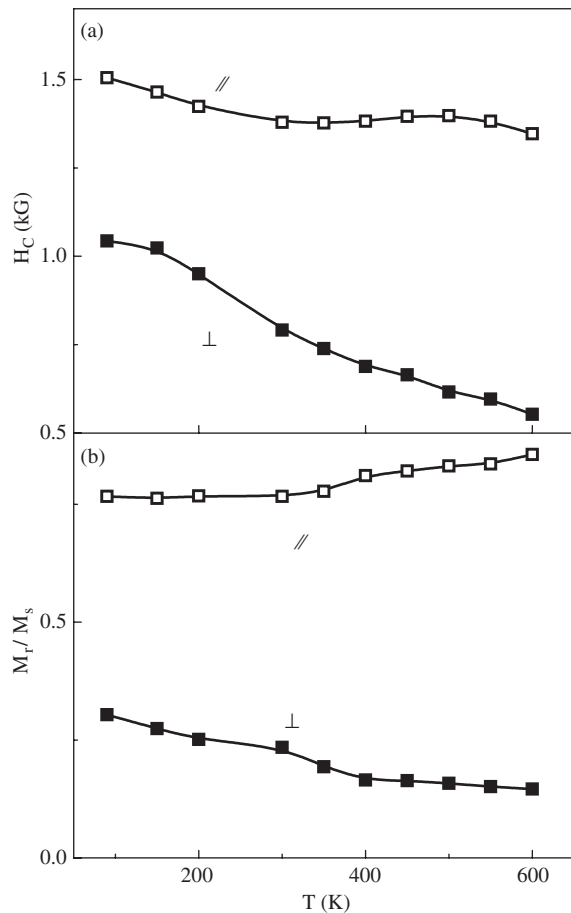


Fig. 4. Temperature dependence of (a) coercive field and (b) remanent ratio in two geometries. The empty and filled boxes refer to the parallel and perpendicular geometries, respectively.

aligned along the wire axis. Fig. 6 shows typical angular dependence of the coercivity and the remanent ratio for the diameter of 40 nm. The coercivity and the remanent ratio change simultaneously with the direction of the applied magnetic field. However, for 80 nm the dependence is quite different. Although the remanent ratio changes in the same way as that of 40 nm, the coercivity does not change much.

In order to explain above experimental results in Figs. 3–6, several aspects must be considered. First, because of the large aspect ratio of Co–Pt nanowires, the shape anisotropy energy $2\pi M_s^2$ is expected to play a dominant role in the effective magnetic anisotropy

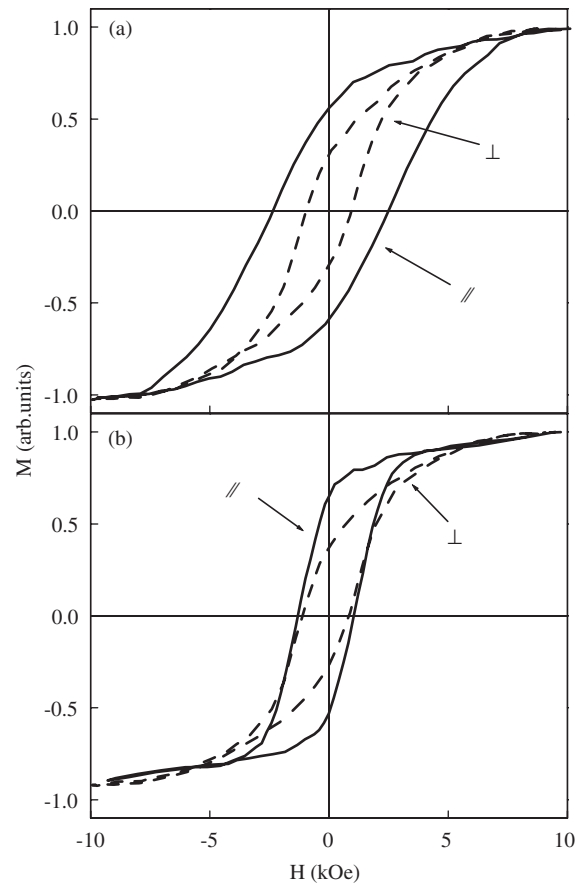


Fig. 5. Magnetization hysteresis loops for an array of (a) 40 nm and (b) 80 nm diameter Co–Pt nanowires in AAO templates. The solid and dash curves refer to the parallel and perpendicular geometries, respectively.

and its easy axis is parallel to the wire axis, where M_s is the saturation magnetization. Secondly, the magnetocrystalline anisotropy must be taken into account. For present Co–Pt nanowires with small diameters, the (111) orientation of most grains and thus the easy axis of the magnetocrystalline anisotropy are also aligned along the nanowire axis. Although the magnetocrystalline anisotropy is in the order of 10^5 erg/cm³, about one order smaller than the demagnetization energy [16], it has an apparent effect on the effective magnetic anisotropy. Finally, since the squareness is still less than one unit for small diameters, magnetostatic interaction between neighboring nanowires should be considered [18].

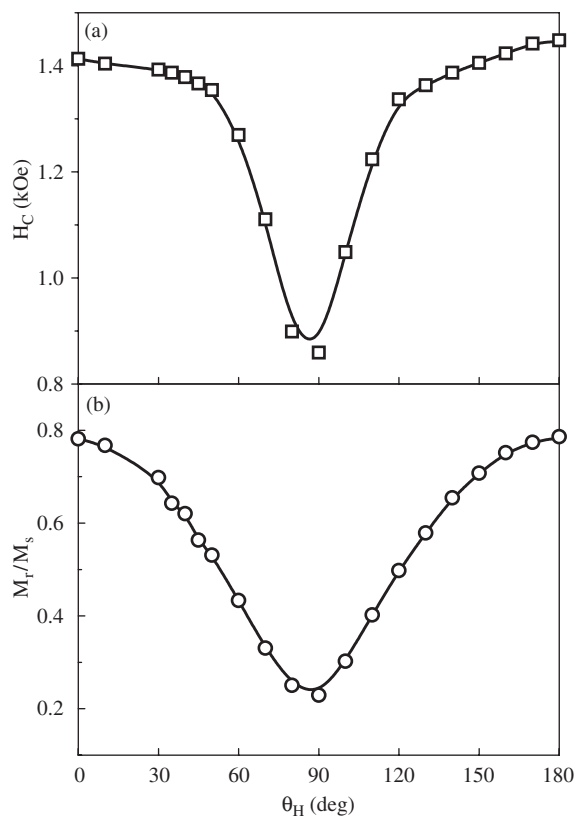


Fig. 6. Angular dependence of (a) coercivity and (b) remanent ratio for the diameter of 40 nm, where θ_H is the angle between the applied magnetic field and the wire axis.

For the present Co–Pt nanowires, the total energy consists of the demagnetization energy E_{de} , the magnetocrystalline anisotropy E_K , and the dipolar magnetostatic interaction energy E_{di} . Here, we have $E_{de}(\parallel) < E_{de}(\perp)$, $E_K(\parallel) < E_K(\perp)$, and $E_{di}(\parallel) > E_{di}(\perp)$, where \parallel refers to the magnetization parallel to the wire axis and \perp to the magnetization perpendicular to the wire axis. For small diameters, the total energy of the nanowires with the magnetization along the wire axis is smaller than that of the perpendicular geometry and the easy axis favors to be aligned along the wire axis. As the voltage is increased during the fabrication of AAO templates, the diameter of pores and the density of pores are increased simultaneously. With the density of pores increasing, the dipolar interaction is increased and the

total energy approaches each other in the two geometries for large diameters [19]. In this case, the easy axis favors to be aligned perpendicular to the wire axis. Therefore, the coercivity in the two geometries crosses as a function of the diameter as shown below. Although the shape anisotropy is the major contribution to the magnetic anisotropy, the evolution of the coercivity and the remanent ratio in the parallel and the perpendicular geometries results from a competition among the shape and magnetocrystalline anisotropies, and the dipolar magnetostatic interactions. The results in Fig. 4 might hint that, as the temperature is lowered, the difference of the dipolar magnetostatic interaction between the parallel and perpendicular geometries is increased more rapidly than those of the magnetocrystalline and the shape anisotropies. It should also be pointed that other reasons cannot be excluded, such as a distribution in the orientations of crystallographic axes and an enhancement of the magnetocrystalline anisotropy in small grains with respect to bulk materials.

For the present Co–Pt nanowires, the room temperature H_C in the parallel and the perpendicular geometries decreases rapidly as the nanowire diameter is increased. When the diameter is increased from 40 to 70 nm for example, H_C in the parallel geometry decreases from 2430 to 870 Oe. Moreover, the difference between the two configurations becomes small with the diameter increasing. More remarkably, Fig. 7 shows that the coercivity in the two geometries scales as a linear function of $1/R^2$, where R is the radius of nanowires. As is well known, for magnetic nanowires the magnetization reversal mechanism strongly depends on the diameter. For a specific material, there is a critical radius R_C , where a transition of coercivity behavior can usually be observed. If $R > R_C$, the magnetization reversal process can be described by curling mode and the coercivity decreases with increasing diameter of nanowires. Using the spin S , Curie temperature T_C and saturation magnetization M_S for bulk Co–Pt alloy, the critical diameter can be estimated [20]. It is smaller than 20 nm in the present case and close to that of 14 nm for $\text{Co}_{0.65}\text{Pt}_{0.35}$ nanowires [16].

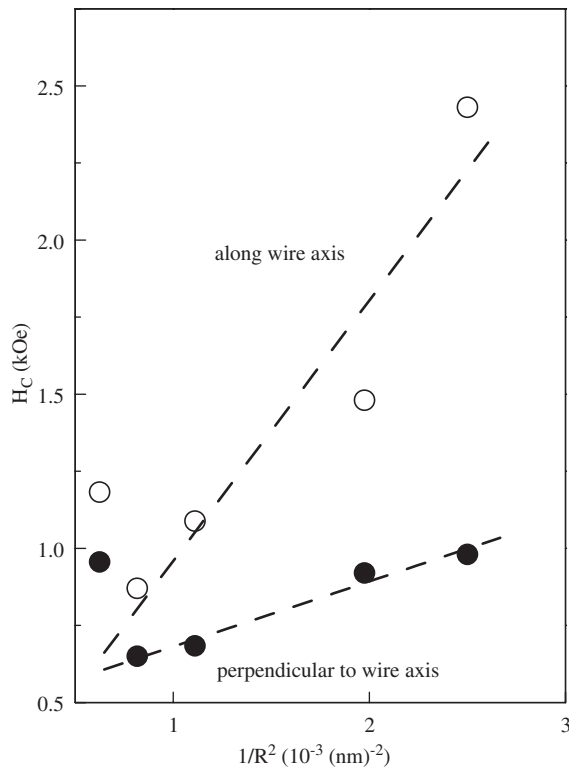


Fig. 7. Dependence of room temperature coercivity on nanowire radius for Co–Pt nanowires in the parallel (○) and perpendicular geometries (●). The dash line corresponds to linear fitting results.

Since the diameter of the present nanowires is much larger than the critical value, the magnetization reversal process is dominated by curling mode. Thus, the H_C of nanowires is given as follows [21]:

$$H_C = \frac{2\pi k A}{M_S} \frac{1}{R^2} + \frac{2K_U}{M_S}, \quad (1)$$

where the right term $2K_U/M_S$ is the magnetocrystalline anisotropy field with uniaxial anisotropy constant K_U . The dependence of the coercivity on the radius in Fig. 7 can be fitted very well using Eq. (1), indicating that the magnetization reversal process can be described by curling mode [22]. As shown in Fig. 7, H_C for 80 nm is larger than that of 70 nm, which may originate from existence of Co component and more random alignment of grain orientations in Co–Pt component as shown

by X-ray measurements in Fig. 2. It coincides with the results in Fig. 5(b).

4. Conclusion

Arrays of Co–Pt nanowires with various diameters have been successfully prepared by electro-deposition into the pores of AAO templates. The as-prepared Co–Pt nanowires were observed by XRD to have FCC structure with preferred orientation of (111) along the nanowire. The coercivity of nanowires in the parallel geometry is larger than that of the perpendicular geometry and approaches each other in the two geometries for large diameters and low-temperatures. These experimental results can be qualitatively explained after taking into account the shape and magneto-crystalline anisotropies, and the dipolar magnetic interaction. Since the diameter is larger than the critical value, the magnetization reversal process can be described by curling mode, and the coercivity in the two geometries decreases with a linear scale of $1/R^2$ as the nanowire diameter is increased. The structure of the nanowires is found to have a strong influence on the magnetic properties.

Acknowledgements

This work was supported by the National Science Foundation of China Grants nos. 10174014, 60271013, 60490290, and 10021001, and the State Key Project of Fundamental Research Grant nos. 2001CB610602 and 2002CB613504, JSNSF, and Shanghai Nanotechnology Program Center (no. 0252nm004).

References

- [1] G.T.A. Huysmans, J.C. Lodder, J. Wakui, J. Appl. Phys. 64 (1988) 2016.
- [2] M. Moskovits, J.M. Xu, IEEE Trans. Magn. 43 (1996) 1646.
- [3] D.J. Sellmyer, M. Zheng, R. Skomski, J. Phys.: Condens. Matter 13 (2001) R433.
- [4] Y. Peng, H.L. Zhang, S.L. Pan, H.L. Li, J. Appl. Phys. 87 (1999) 7405.

- [5] Z.Y. Chen, Q.F. Zhan, D.S. Xue, F.S. Li, H. Kunkel, G. Williams, *J. Phys.: Condens. Matter* 14 (2002) 613.
- [6] X.Y. Zhang, G.H. Wen, Y.F. Chan, R.K. Zheng, X.X. Zhang, N. Wang, *Appl. Phys. Lett.* 83 (2003) 3341.
- [7] R. Skomski, H. Zeng, M. Zheng, D.J. Sellmyer, *Phys. Rev. B* 62 (2000) 3900.
- [8] L. Sun, P.C. Searson, C.L. Chien, *Phys. Rev. B* 61 (2000) R6463.
- [9] Q.F. Zhan, Z.Y. Chen, D.S. Xue, F.S. Li, H. Kunkel, X.Z. Zhou, R. Roshko, G. Williams, *Phys. Rev. B* 66 (2002) 134436.
- [10] Q.F. Liu, C.X. Gao, J.J. Xiao, D.S. Xue, *J. Magn. Magn. Mater.* 260 (2003) 151.
- [11] Y.H. Huang, H. Okumura, G.C. Hadjipanayis, D. Weller, *J. Appl. Phys.* 91 (2002) 6869.
- [12] S. Shiomi, H. Okazawa, T. Nakakita, T. Kobayashi, M. Masuda, *Jpn. J. Appl. Phys.* 32 (3A) (1993) L315; L. Uba, S. Uba, V.N. Antonov, A.N. Yaresko, R. Gontarz, *Phys. Rev. B* 64 (2001) 125105.
- [13] D. Weller, H. Brandle, C. Chappert, *J. Magn. Magn. Mater.* 121 (1993) 461.
- [14] C.N. Chinnasamy, B. Jeyadevan, K. Shinoda, K. Tohji, *J. Appl. Phys.* 93 (2003) 7583.
- [15] N. Yasui, A. Imada, T. Den, *Appl. Phys. Lett.* 83 (2003) 3347.
- [16] I. Mallet, K.Y. Zhang, C.L. Chien, T.S. Egleton, P.C. Searson, *Appl. Phys. Lett.* 84 (2004) 3900.
- [17] P.M. Paulus, F. Luis, M. Kröll, G. Schmid, L.J. de Jongh, *J. Magn. Magn. Mater.* 224 (2001) 180.
- [18] V. Raposo, J.M. Garcia, J.M. González, M. Vazquez, *J. Magn. Magn. Mater.* 222 (2000) 227.
- [19] J. Rivas, A.K.M. Bantu, G. Zaragoza, M.C. Blanco, M.A. López-Quintela, *J. Magn. Magn. Mater.* 249 (2002) 220.
- [20] M. Zheng, L. Menon, H. Zeng, Y. Liu, S. Bandyopadhyay, R.D. Kirby, D.J. Sellmyer, *Phys. Rev. B* 62 (2000) 12282.
- [21] H. Zeng, R. Skomski, L. Menon, Y. Liu, S. Bandyopadhyay, D.J. Sellmyer, *Phys. Rev. B* 65 (2002) 134426.
- [22] A. Aharoni, *J. Appl. Phys. (Suppl.)* 30 (1959) 70S.